This is the Pre-Published Version.

https://dx.doi.org/10.1016/j.optlaseng.2020.106453

Wavefront control through multi-layer scattering media using single-pixel detector for high-PSNR optical transmission

Yin Xiao, Lina Zhou, Wen Chen*

Department of Electronic and Information Engineering, The Hong Kong Polytechnic University, Hong Kong, China

*Corresponding author: owen.chen@polyu.edu.hk

Abstract: We propose a new approach for optical analog-signal transmission through multi-layer scattering media using single-pixel detector to achieve high peak signal-to-noise ratio (PSNR), and analog signals can be experimentally received with high PSNR through multi-layer scattering media. The proposed approach, experimental observation and optical experimental results are presented that intensity of the propagating wave recorded by using single-pixel detector can directly produce high-PSNR signals through multi-layer scattering media using coherent light source at the receiving end. In our optical experiments, high-PSNR optical transmission is realized in different wave propagation environments, e.g., multi-layer scattering media. The observed phenomenon and the proposed approach provide a new and interesting insight about optical analog-signal transmission through multi-layer scattering media. @ Elsevier.

Keywords: Optical transmission, high-SNR analog-signal retrieval, scattering media.

I. Introduction

Optical wave has been extensively studied for data transmission over the past decades [1–4]. Optical fiber is a prime means for transmitting digital signals nowadays, and has been widely used in the field of communications [5–8]. It is meaningful and significant to exploit effective methods to transmit analog signals by using optical waves (especially in the visible spectrum range) in free space. However, scattering media or blockades existing in free space strongly destroy the desired wave (i.e., information carrier) by the light scattering or reflection [9–15]. Multi-layer scattering also breaks down Fresnel or Fraunhofer diffraction theory, making it difficult to control wave propagation in complex environments. As a result, realizing optical transmission with high peak signal-to-noise ratio (PSNR) in complex environments is considered to be optically difficult, which limits the further development of optical transmission. Coherent light source (e.g., laser) has a stable frequency and phase, which is suitable for long distance transmission. However, when coherent light source is used, the noise, e.g., speckle noise, is usually inevitable, which always acts as strong background noise at the receiving end. Hence, it is highly desirable to explore a method which can utilize the coherent light source to transmit the desired analog data through scattering media and simultaneously suppress the noise dramatically.

Furthermore, in terms of optical information carrier, no study utilizes random amplitude-only patterns to transmit analog signals. Although the series of random amplitude-only patterns can be easily generated and used [16–19], they are not effectively implemented as information carrier due to the lack of controllability. In this case, the background is always noisy and the PSNR of the retrieved data is low. Hence, it is also a significant challenge to achieve high-quality transmission through scattering media by using random amplitude-only patterns. It is significant and meaningful to explore a method which can retrieve the analog data with high robustness against noise when coherent light source and a series of random amplitude patterns are applied. In addition, no method has been developed before to directly realize high-PSNR optical transmission in various wave propagation environments, e.g., multi-layer scattering media. From the perspective of optical transmission, there is a fundamental limit that the analog data cannot be transmitted through multi-layer scattering media with high PSNR.

In this paper, we propose a new approach to controlling wavefront for high-PSNR optical transmission through multi-layer scattering media by using coherent light source and a series of random amplitude-only patterns. This new approach is capable of directly retrieving the analog signals with high PSNR at the receiving end even through multi-layer scattering media by using coherent light source, and is highly robust against the noise existing in various wave propagation environments. At the receiving end, single-pixel detector is used to collect intensity of the propagating wave. The potential benefits of applying single-pixel detector include its low cost and high capability under the conditions of non-visible wavelength band (e.g., X-ray [20,21] and terahertz light [22–24]) and various environments [25–27]. It is demonstrated in optical experiments that the proposed method shows high transmission reliability in various wave propagation environments.

© 2020. This manuscript version is made available under the CC-BY-NC-ND 4.0 license http://creativecommons.org/licenses/by-nc-nd/4.0/.

2. Principle

A schematic experimental setup for the proposed high-PSNR optical analog-signal transmission is shown in Fig. 1, where a series of generated random amplitude-only patterns as information carrier are sequentially embedded and illuminated to propagate through scattering media (e.g., three cascaded diffusers) and then the intensity values recorded by single-pixel detector can directly produce the analog data with high PSNR at the receiving end.

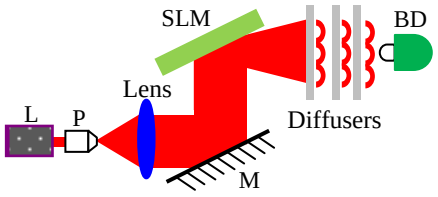

Fig. 1. A schematic experimental setup for the proposed high-PSNR optical analog-signal transmission through transmissive and opaque scattering media: L: He-Ne laser; P: Pinhole; M: Mirror; BD, Bucket detector (i.e., single-pixel detector); SLM, Spatial light modulator.

In the proposed optical transmission architecture, original analog data is used as a series of independent pixels, and each pixel value is transformed or theoretically mapped to one random amplitude-only pattern according to the proposed procedure as follows: (1) generate and initialize a random amplitude-only pattern with real values; (2) apply Fourier transform (FT) to the generated random amplitude-only pattern and obtain its Fourier spectrum; (3) use one pixel value of original analog data to replace zero-frequency component of the generated Fourier spectrum, and obtain a new Fourier spectrum; (4) apply inverse Fourier transform (IFT) to the new Fourier spectrum to generate an updated random amplitude-only pattern. Each pixel of original analog data is sequentially processed by using the aforementioned procedure, therefore a series of random amplitude-only patterns can be correspondingly generated as information carrier. A flow chart for generating the random amplitude-only patterns is shown in Fig. 2.

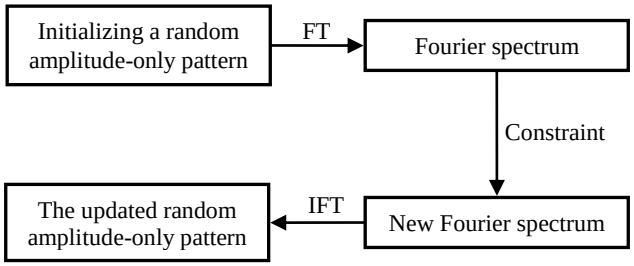

Fig. 2. Flow chart for generating random amplitude-only patterns.

The Fourier spectrum of any real matrix (i.e., matrix with real values) is a symmetric complex matrix [28]. The only one real value locates at the center of the generated Fourier spectrum, i.e., zero-frequency component. When the zero-frequency component is replaced by other real value, the updated Fourier spectrum is a new symmetric complex matrix and the IFT of this new symmetric complex matrix leads to an updated real matrix. Hence, each pixel value of original data can be theoretically mapped to one 2D random amplitude-only pattern in the proposed method. When the pattern is illuminated to propagate in free space, according to the Huygens-Fresnel principle, every point on a wavefront is a source of wavelets, which means that the form of the wave at any subsequent time is determined by the sum of these secondary waves. In the proposed method, at wave propagation path, each point in free space contains original information of the encoded pixel according to Huygens-Fresnel principle. This property has been fully utilized in the proposed method to optically transmit information through scattering media.

After the transformation in spatial and frequency domains, the finally generated amplitude-only pattern can be described by

$$\begin{aligned} B&=\iint P(x,y)e^{-2\pi j(x\xi+y\eta)}dxdy\big|_{\xi=0,\eta=0} \\ &=\iint P(x,y)dxdy \end{aligned}, \qquad (1)$$

where $j=\sqrt{-1}$, $P(x,y)$ denotes the finally generated random amplitude-only pattern, (x,y) denotes the coordinate in spatial domain, (ξ,η) denotes the coordinate in frequency domain, and B denotes the zero-frequency component which is equivalent to each pixel value of the analog data. It can be found that Eq. (1) corresponds to the single-pixel detection process in free space. The generated amplitude-only patterns serve as information carrier. Although each pixel value of the analog signal is theoretically mapped to one 2D random amplitude-only pattern in free space, it is experimentally observed that the generated amplitude-only patterns can be used for high-PSNR data transmission in various wave propagation environments, e.g., through multi-layer scattering media. Size of the generated amplitude-only pattern can be flexibly adjusted in practice, and is not limited by original data. For instance, if the data has a size of 64×64 pixels, each pixel value of the data can be theoretically mapped to one random amplitude-only pattern with any other size, e.g., 128×128 or 256×256 pixels.

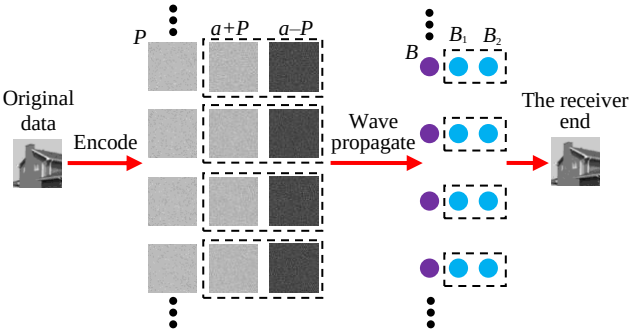

Fig. 3. A schematic process for the proposed high-PSNR optical analog-signal transmission: a denotes a constant, B_1 corresponds to $(a+p)$, B_2 corresponds to $(a–p)$, and $B=B_1–B_2$. The dashed boxes given here are used to represent those to be practically implemented in optical experiments. Here, free space, transmissive scattering media and reflective scattering media are individually studied as wave propagation environment.

It is experimentally observed that the proposed high-PSNR optical transmission can be realized even through multi-layer scattering media, and the intensity recorded by the single-pixel detector can be used to directly retrieve the analog data with high PSNR at the receiving end. This is a key feature of the proposed high-PSNR optical transmission method. A schematic process for the proposed high-PSNR optical transmission is shown in Fig. 3. Original analog data is first encoded into a series of random amplitude-only patterns $P(x,y)$ according to the proposed principle. Subsequently, three wave propagation environments, i.e., free space, reflective scattering media and transmissive scattering media, are individually studied and tested. A series of intensity values can be sequentially recorded by the single-pixel bucket detector, schematically illustrated in Figs. 1 and 3. At the receiving end, intensity values recorded by the single-pixel detector are used to directly retrieve the high-PSNR data without additional post-processing algorithms.

In the optical experiments, the series of random amplitude-only patterns $P(x,y)$ used for high-PSNR transmission is first generated. The generated amplitude-only patterns contain negative values which cannot be directly used in optical experiments. Here, each generated amplitude-only pattern $P(x,y)$ is simply converted into two random amplitude-only patterns as schematically illustrated in Fig. 3, i.e., $a+P$ and $a–P$ where a denotes a constant to avoid negative values. Therefore, for each pixel of original analog data, two amplitude-only patterns are experimentally used and sequentially embedded into the SLM as shown in Fig. 1. In the wave propagation environment, B_1 denotes one intensity value recorded by single-pixel detector corresponding to pattern ($a+P$), and B_2 denotes one intensity value recorded by the single-pixel detector corresponding to pattern ($a–P$), schematically illustrated in Fig. 3. Therefore, the intensity value ($B=B_1–B_2$) proportionally corresponds to each pixel value of original analog data. The objectives to use two amplitude-only patterns as information carrier for optically transmitting each pixel of the analog data are: (1) negative values of the generated amplitude-only patterns can be fully avoided in optical experiments; (2) the noise existing in optical experiments can be fully suppressed. For instance, when the two amplitude-only patterns sequentially embedded into the SLM are illuminated by coherent light source, the intensity value ($B_1–B_2$) has a strong relationship with one pixel value of the original analog data. It is found in our optical experiments that intensity value ($B_1–B_2$) is proportional to the pixel value of original analog data, which means that there is a scaling factor between the retrieved intensity value ($B_1–B_2$) and pixel value of original analog data. It is also observed that the scaling factors are within a very small range in each wave propagation environment, and have no effect on the high-PSNR information retrieval at the receiving end.

3. Experimental results and discussion

Optical experiments have been carried out, and experimental results are observed and presented to illustrate the proposed high-PSNR optical analog-signal transmission. First, through transmissive and opaque scattering media, a typical experimental setup is shown in Fig. 1, where coherent light source (i.e., He-Ne laser, 17.0 mW) with wavelength of 633.0nm is expanded by a pinhole and collimated by a lens with focal length of 100.0mm. In practice, the light source with other wavelengths can also be applicable. The collimated light source illuminates the SLM (Holoeye, LC-R720) with pixel size of 20.0μm and the generated random amplitude-only patterns ($a+P$) and ($a–P$) are sequentially embedded and illuminated to propagate through scattering media. Three wave propagation environments are presented here, i.e., free space, through one diffuser and through three cascaded diffusers. Experimental results of the high-PSNR transmission and retrieval are shown in Figs. 4(a)–4(r) respectively for the three different wave propagation environments. In Figs. 4(a)–4(r), multiple sets of analog data have been individually tested in each wave propagation environment. The PSNR values are calculated to quantitatively evaluate quality of the retrieved data. Mean squared error (MSE) is also used to compare the difference between the retrieved data and original data, which is defined as the average squared difference between the pixel values of retrieved data and the pixel values of original data. The PSNR and MSE values for the retrieved data in different wave propagation environments are given in Fig. 4.

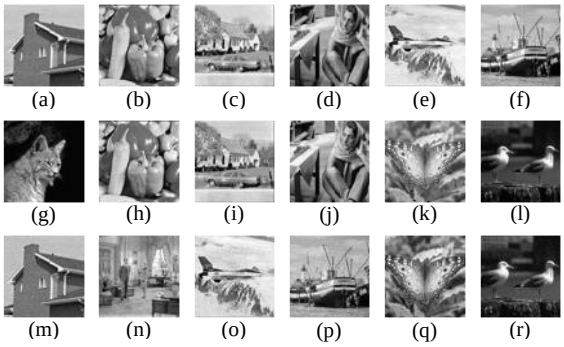

Fig. 4. Optical experimental results obtained at the receiving end: (a)–(f) Analog data (64×64 pixels) experimentally retrieved by using single-pixel detector in the wave propagation environment without any diffuser (i.e., free space) in Fig. 1, with the PSNR values respectively of 37.39 dB, 38.29 dB, 33.37 dB, 35.41 dB, 36.74 dB and 38.51 dB, with the MSE values respectively of 1.82×10^{-4}, 1.48×10^{-4}, 4.60×10^{-4}, 2.88×10^{-4}, 2.12×10^{-4} and 1.41×10^{-4}. (g)–(l) Analog data (64×64 pixels) experimentally retrieved by using single-pixel detector in the wave propagation environment with only one diffuser placed in the optical setup in Fig. 1, with the PSNR values respectively of 41.88 dB, 39.02 dB, 38.31 dB, 37.63 dB, 35.94 dB and 44.09 dB, with the MSE values respectively of 6.48×10^{-5}, 1.25×10^{-4}, 1.47×10^{-4}, 1.73×10^{-4}, 2.55×10^{-4} and 3.89×10^{-5}. (m)–(r) Analog data (64×64 pixels) experimentally retrieved by using single-pixel detector in the wave propagation environment with three cascaded diffusers placed in the optical setup in Fig. 1, with the PSNR values respectively of 31.67 dB, 36.72 dB, 36.13 dB, 31.26 dB, 34.63 dB and 36.71 dB, with the MSE values respectively of 6.80×10^{-4}, 2.13×10^{-4}, 2.59×10^{-4}, 7.49×10^{-4}, 3.45×10^{-4} and 2.08×10^{-4}. It is worth noting that multiple sets of analog signals have been individually tested and transmitted in each wave propagation environment.

The experimental results shown in Figs. 4(a)–4(f) are obtained in free space without any diffuser placed in the

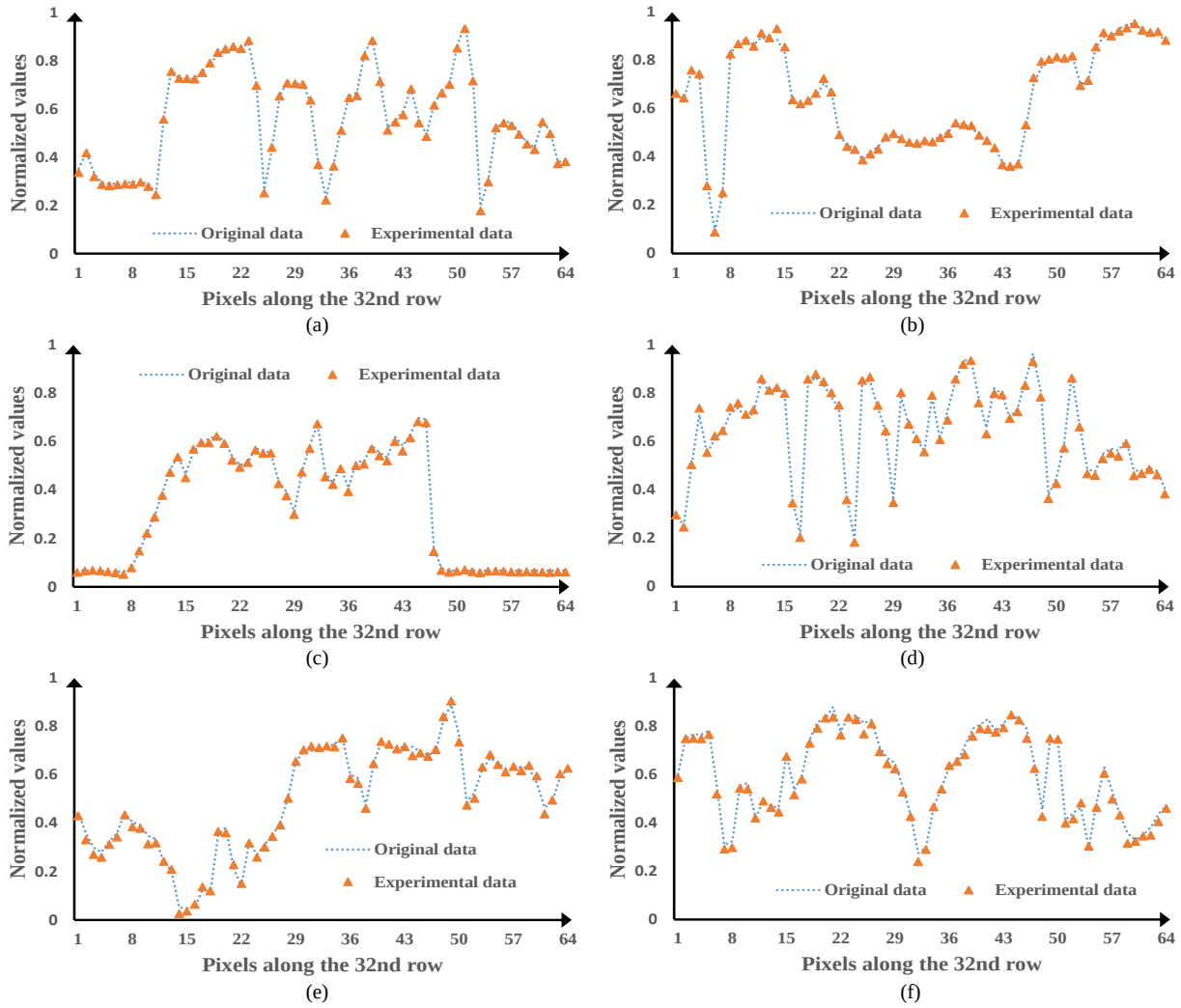

Fig. 5. Typical comparisons between the experimentally received data and original analog data: (a) A comparison between the pixel values along the 32nd row of Fig. 4(b) and those in original analog data when no diffuser is placed in the optical setup in Fig. 1, (b) a comparison between the pixel values along the 32nd row of Fig. 4(e) and those in original analog data when no diffuser is placed in the optical setup in Fig. 1, (c) a comparison between the pixel values along the 32nd row of Fig. 4(g) and those in original analog data when one diffuser is placed in the optical setup in Fig. 1, (d) a comparison between the pixel values along the 32nd row of Fig. 4(i) and those in original analog data when one diffuser is placed in the optical setup in Fig. 1, (e) a comparison between the pixel values along the 32nd row of Fig. 4(n) and those in original analog data when three cascaded diffusers are placed in the optical setup in Fig. 1, and (f) a comparison between the pixel values along the 32nd row of Fig. 4(q) and those in original analog data when three cascaded diffusers are placed in the optical setup in Fig. 1.

optical setup in Fig. 1, and the intensity values are recorded by using a single-pixel detector (Newport, 918D-UV-OD3R). The experimental results shown in Figs. 4(g)–4(l) are obtained, when one diffuser (Thorlabs, DG10-1500) with the diameter of 25.4 mm and thickness of 2.0 mm is placed in the optical setup in Fig. 1. In a strongly scattering environment with three cascaded diffusers, it is experimentally observed that the high-PSNR data can also be obtained, as shown in Figs. 4(m)–4(r). In Fig. 1, axial distance between the first diffuser and the second diffuser is 25.0 mm, and axial distance between the second diffuser and the third diffuser is 10.0 mm. In the proposed high-PSNR optical transmission, there is also no limitation about the axial distances, e.g., between the diffuser and the single-pixel detector. In our experiments, the axial distance between the final diffuser and the single-pixel detector is set as 3.5 cm. It is observed from Figs. 4(a)–4(r) that the analog data retrieved at the receiving end is always of high quality in different wave propagation environments, which is clearly verified by the calculated PSNR and MSE values given in Fig. 4. Even in a strongly scattering environment, when the series of random amplitude-only patterns and coherent light source are applied, the proposed high-PSNR optical transmission is also realized. Hence, the proposed method possesses high robustness in different environments, which means that different layers of scattering media would have little influence on the measured results**.** It is worth noting that various types of data, e.g., analog signals, can be transmitted by using the proposed method.

To further illustrate the relationship between the pixel values of experimentally retrieved data and pixel values of original analog data, the pixel values along the 32nd row of Figs. 4(b), 4(e), 4(g), 4(i), 4(n) and 4(q) and those in original analog data are compared. As can be seen from the typical comparisons in Figs. 5(a)–5(f), the experimental data almost

overlap with pixel values of original analog data after the normalization operation. Here, to conduct normalization, all experimental data are divided by the maximum value of experimental data, and for original signal all values are divided by the maximum value of original signal. It is demonstrated that high-PSNR optical transmission through multi-layer scattering media is realized and observed.

High-PSNR optical transmission and retrieval through reflective scattering media are also studied and observed. A typical experimental setup is shown in Fig. 6. In the reflective scattering environment, an ordinary paper serves as a reflective scattering medium, and a series of the generated random amplitude-only patterns are sequentially embedded into the SLM. The single-pixel detector records the light intensity reflected from the paper.

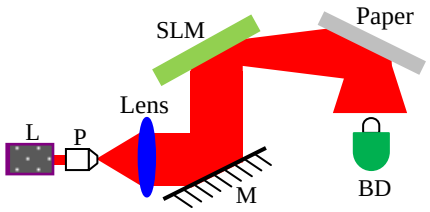

Fig. 6. A schematic experimental setup for the proposed high-PSNR optical analog-signal transmission through reflective scattering media: an ordinary paper is placed just before a plate as reflective scattering media.

Optical experimental results, i.e., the retrieved data, are shown in Figs. 7(a)–7(f). In Figs. 7(a)–7(f), multiple sets of analog data have been individually tested. The PSNR values and the MSE values of the retrieved data are shown in Fig. 7. The pixel values along the 32nd row of Figs. 7(a), 7(c) and 7(f) and those in original analog data are compared and respectively shown in Figs. 7(g)–7(i) to illustrate high-PSNR optical transmission. It is always observed that high-PSNR optical transmission and retrieval through reflective scattering media can also be realized.

Based on experimental results in Figs. 5 and 7, the proposed method provides a powerful tool to address practical applications. For instance, it is still a great challenge to use visible and coherent light source to realize high-fidelity optical data transmission where blockade, reflection and scattering could occur, and quality of the information retrieved at the receiving end is significantly affected. The proposed method resolves the problems encountered in data transmission.

It is also experimentally found that in each wave propagation environment, there are steady scaling factors between the pixel values of retrieved data and those in original analog data. The typical results about scaling factors are shown in Figs. 8(a)–8(d), i.e., corresponding to the optical setups in free space, through one diffuser, through three cascaded diffusers, and through reflective scattering media with the experimental results respectively in Figs. 4(b), 4(l), 4(m) and 7(f). The scaling factor is calculated by the ratio between the retrieved intensity values ($B=B_1-B_2$) and pixel values of original analog data. As seen in Figs. 8(a)–8(d), in each wave propagation environment, the scaling factors are within a very small range. It is demonstrated again that in each wave propagation environment, the proposed high-PSNR optical transmission through scattering media is realized and observed.

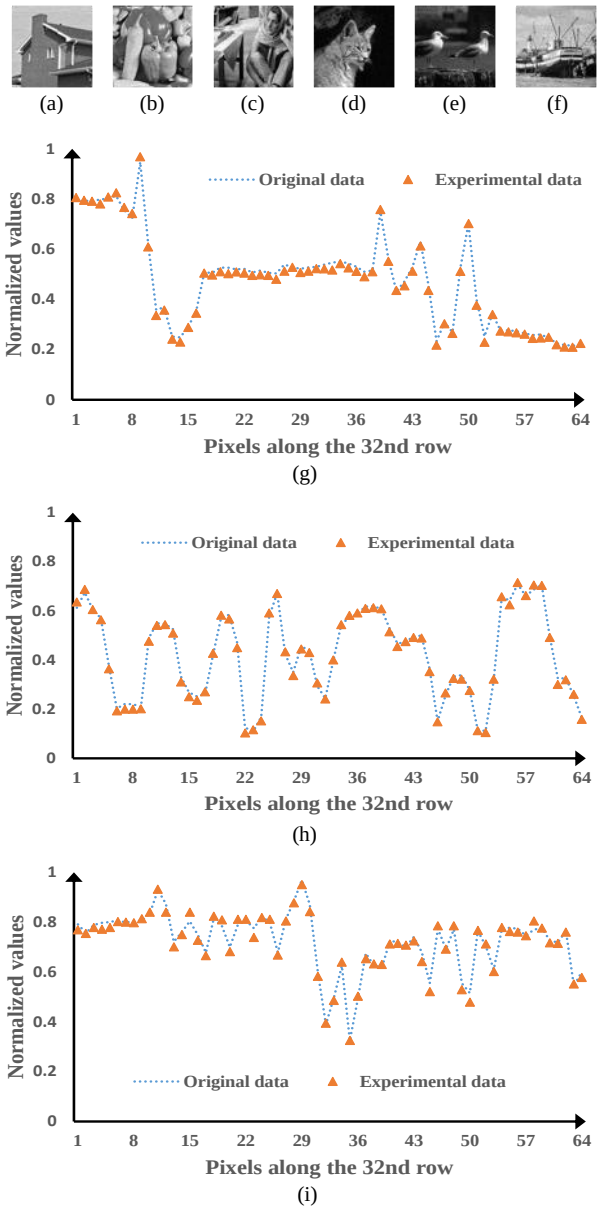

Fig. 7. Optical experimental results obtained at the receiving end: (a)–(f) The analog data (64×64 pixels) experimentally retrieved by using single-pixel detector in optical experiments, with the PSNR values respectively of 38.64 dB, 35.95 dB, 34.97 dB, 39.22 dB, 36.70 dB and 34.72 dB, with the MSE values respectively of 1.37×10^{-4}, 2.54×10^{-4}, 3.19×10^{-4}, 1.20×10^{-4}, 2.13×10^{-4} and 3.37×10^{-4}, (g) a comparison between the pixel values along the 32nd row of (a) and those in original analog data, (h) a comparison between the pixel values along the 32nd row of (c) and those in original analog data, and (i) a comparison between the pixel values along the 32nd row of (f) and those in original analog data. Multiple sets of analog data have been individually tested and transmitted through reflective scattering media.

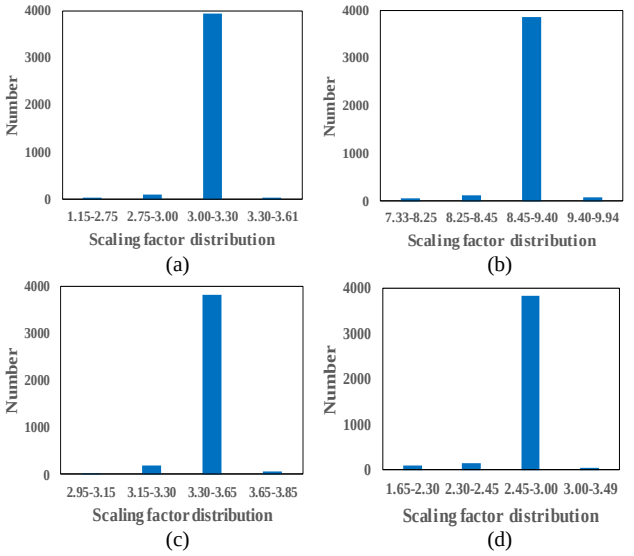

Fig. 8. Typical scaling factor distributions obtained in different wave propagation environments: (a) The scaling factor distribution (magnitude of the coefficients: 10^{-11}) obtained corresponding to the experimental result in Fig. 4(b) when the optical setup in Fig. 1 contains no diffuser, (b) scaling factor distribution (magnitude of the coefficients: 10^{-12}) obtained corresponding to the experimental result in Fig. 4(l) when the optical setup in Fig. 1 contains one diffuser, (c) scaling factor distribution (magnitude of the coefficients: 10^{-12}) obtained corresponding to the experimental result in Fig. 4(m) when the optical setup in Fig. 1 contains three cascaded diffusers, and (d) scaling factor distribution (magnitude of the coefficients: 10^{-12}) obtained corresponding to the experimental result in Fig. 7(f) when the optical setup in Fig. 6 contains the reflective scattering medium.

4. Conclusions

We have proposed a new method to transmit and retrieve analog signals with high PSNR through multi-layer scattering media when coherent light source and a series of random amplitude-only patterns as information carrier are applied. In our optical experiments, high-PSNR optical transmission has been realized and observed in different wave propagation environments, i.e., free space, transmissive scattering media, reflective scattering media and multi-layer scattering media.

Disclosures

The authors declare that there are no conflicts of interest.

REFERENCES

[1] Seeds AJ and Williams KJ. Microwave photonics. J Lightw Technol 2006;24(12):4628-41.

[2] Capmany J and Novak D. Microwave photonics combines two worlds. Nat Photonics 2007;1:319–30.

[3] Koenig S, Lopez-Diaz D, Antes J, Boes F, Henneberger R, Leuther A, Tessmann A, Schmogrow R, Hillerkuss D, Palmer R, Zwick T, Koos C, Freude W, Ambacher O, Leuthold J, and Kallfass I. Wireless sub-THz communication system with high data rate. Nat Photonics 2013;7:977–81.

[4] Nagatsuma T, Ducournau G, and Renaud CC. Advances in terahertz communications accelerated by photonics. Nat Photonics 2016;10:371–9.

[5] Bozinovic N, Yue Y, Ren YX, Tur M, Kristensen P, Huang H, Willner AE, and Ramachandran S. Terabit-scale orbital angular momentum mode division multiplexing in fibers. Science 2013;340(6140):1545–8.

[6] Ramachandran S and Kristensen P. Optical vortices in fiber. Nanophotonics 2013;2(5-6):455–74.

[7] Ndagano B, Brüning R, McLaren M, Duparré M, and Forbes A. Fiber propagation of vector modes. Opt. Express 2015;23(13):17330–6.

[8] Zhu L, Liu J, Mo Q, Du C, and Wang J. Encoding/decoding using superpositions of spatial modes for image transfer in km-scale few-mode fiber. Opt. Express 2016;24(15):16934–44.

[9] Bertolotti J, van Putten EG, Blum C, Lagendijk A, Vos WL, and Mosk AP. Non-invasive imaging through opaque scattering layers. Nature 2012;491:232–4.

[10] Popoff SM, Lerosey G, Fink M, Boccara AC, and Gigan S. Image transmission through an opaque material. Nat Commun 2010;1:81.

[11] Katz O, Small E, and Silberberg Y. Looking around corners and through thin turbid layers in real time with scattered incoherent light. Nat Photonics 2012; 6,:549–53.

[12] Luo YQ, Yan SX, Li HH, Lai PX, and Zheng YJ. Focusing light through scattering media by reinforced hybrid algorithms. APL Photonics 2020;5(1):016109.

[13] Park JH, Yu ZP, Lee KR, Lai PX, and Park YK. Perspective: Wavefront shaping techniques for controlling multiple light scattering in biological tissues: Toward in vivo applications. APL Photonics 2018;3(10):100901.

[14] Sheng P. Introduction to Wave Scattering, Localization and Mesoscopic Phenomena, Academic, 1995.

[15] Chen XD. Computational Methods for Electromagnetic Inverse Scattering, Wiley-IEEE, 2018.

[16] Bennink RS, Bentley SJ, and Boyd RW. “Two-photon” coincidence imaging with a classical source. Phys Rev Lett 2002;89(11):113601.

[17] Gatti A, Brambilla E, Bache M, and Lugiato LA. Ghost imaging with thermal light: comparing entanglement and classical correlation. Phys Rev Lett 2004;93(9):93602.

[18] Jeffrey HS. Computational ghost imaging. Phys Rev A 2008;78(6):061802(R).

[19] Bromberg Y, Katz O, and Silberberg Y. Ghost imaging with a single detector. Phys Rev A 2009;79(5):053840.

[20] Pelliccia D, Rack A, Scheel M, Cantelli V, and Paganin DM. Experimental X-ray ghost imaging. Phys Rev Lett 2016;117(11):113902.

[21] Yu H, Lu RH, Han SS, Xie HL, Du GH, Xiao TQ, and Zhu DM. Fourier-transform ghost imaging with hard X rays. Phys Rev Lett 2016;117(11):113901.

[22] Watts CM, Shrekenhamer D, Montoya J, Lipworth G, Hunt J, Sleasman T, Krishna S, Smith DR, and Padilla WJ. Terahertz compressive imaging with metamaterial spatial light modulators. Nat Photonics 2014;8:605-9.

[23] Chan WL, Charan K, Takhar D, Kelly KF, Baraniuk RG, and Mittleman DM. A single-pixel terahertz imaging system based on compressed sensing. Appl Phys Lett 2008;93(12):121105.

[24] Stantchev RI, Sun BQ, Hornett SM, Hobson PA, Gibson GM, Padgett MJ, and Hendry E. Noninvasive, near-field terahertz imaging of hidden objects using a single-pixel detector. Sci Adv 2016;2(6):e1600190.

[25] Zhang P, Gong W, Shen X, and Han S. Correlated imaging through atmospheric turbulence. Phys Rev A 2010;82(3):033817.

[26] Meyers RE, Deacon KS, and Shih Y. Turbulence-free ghost imaging. Appl Phys Lett 2011;98(11):111115.

[27] Bina M, Magatti D, Molteni M, Gatti A, Lugiato LA, and Ferri F. Backscattering differential ghost imaging in turbid media. Phys Rev Lett 2013;110(8):083901.

[28] Goodman JW. Introduction to Fourier Optics, 2nd ed., New York, McGraw-Hill, 1996.